UNIVERSITY OF CALIFORNIA, SAN DIEGO

Elucidating the role of autophagy in the clearance of phosphorylated tau protein in human neurons

A thesis submitted in partial satisfaction of the requirements
for the degree of Master of Science

in

Biology

by

Peter Lotfy

Committee in Charge:

Professor Lawrence Goldstein, Chair
Professor Nicholas Spitzer, Co-Chair
Professor David Traver

2016

The Thesis of Peter Lotfy is approved and it is acceptable in quality and form for publication on microfilm and electronically:

Co-Chair

Chair

University of California, San Diego

2016

DEDICATION

I dedicate this thesis to my mother, for her unbelievable strength, unconditional love, support, and encouragement.

TABLE OF CONTENTS

LIST OF FIGURES

LIST OF TABLES

ACKNOWLEDGEMENTS

First and foremost, I would like to express my gratitude to Dr. Larry Goldstein for allowing me to join the lab and participate in what has been the most rewarding learning experience of my life. My time in the lab has not only introduced me to the field of biomedical research, but has also motivated me to pursue a career in the biomedical sciences. Dr. Goldstein's continued support and guidance has been pivotal in my growth as a student.

I would also like to thank Dr. David Traver and Dr. Nick Spitzer for taking the time to serve as members of my thesis committee. Each has played a significant role in sparking my interest in basic science and neurobiology research, and to both I am greatly indebted.

Next, I would like to thank Dr. John Steele for his mentorship and guidance throughout the past two years. John's exceptional intelligence, patience, and kindness were key in facilitating my growth as a scientist and as a person; I am forever grateful. Next, I would like to thank all the members of the Goldstein lab. To spend my time in such a healthy work environment with supportive and hard-working people was key to the success of this thesis. I will cherish my time here forever. I would especially like to thank Dr. Angels Almenar for her positive energy and for engaging me in random scientific discourse, Cheryl Herrera for bringing me into the lab, Jordan Dizon for her assistance, Dr. Paulina Ordonez for her willingness to teach and to lend a hand (or Laura's), Laura Cabebe for helping me with my immunofluorescence imaging, and Irune Guerra for performing some of the early work on characterizing pCW-Cas9. I

would also like to thank Dr. Ella Tour for her assistance in the preparation of this written thesis.

Lastly, I would like to thank all my friends for their continual support and encouragement while I worked towards this graduate degree. Their positive energy was instrumental in maintaining my motivation and fire throughout these past two years. Finally, I would like to thank my mother for her inspiration, love, and support. This thesis would not have been possible without her.

ABSTRACT OF THE THESIS

Elucidating the role of autophagy in the clearance of phosphorylated tau protein in human neurons

by

Peter Lotfy

Master of Science in Biology

University of California, San Diego, 2016

Professor Lawrence Goldstein, Chair

Professor Nicholas Spitzer, Co-Chair

More than 40 million people world-wide suffer from tauopathies– neurodegenerative diseases in which the aggregation of microtubule-associated protein tau into intracellular inclusions is a core pathology. Recent studies have shown that the ubiquitin-proteasome system (UPS) and the autophagy pathway are responsible for the normal turnover of tau in neurons. Autophagy is a conserved cellular mechanism that is

essential for neuronal homeostasis and impaired as a result of aging, which is the primary risk factor for most tauopathies.

Thus, we hypothesized that dysfunctions in the autophagy pathway impair turnover of tau, and thus facilitate pathogenic aggregation. To test this hypothesis, we first treated human induced pluripotent stem cell (hiPSC)-derived neurons with two compounds that have been shown to promote autophagy, and found that these compounds decreased levels of phosphorylated tau protein, suggesting that autophagy may mediate homeostatic clearance of phospho-tau in human neurons. We also found that inhibition of the UPS induces autophagy and promotes the clearance of both phospho-tau and total tau non-selectively.

In order to identify whether autophagy truly regulates the clearance of phosphorylated tau, we set out to establish a CRISPR/Cas9-based system that would allow us to disrupt autophagy in an efficient and inducible fashion. We have characterized two inducible systems, gathering a foundational understanding of how the system can be applied to genetic screens in hiPSC-derived cell types. Thus, this study both expands on the current knowledge regarding degradation of tau in human neurons and lays the groundwork for further genetic studies using an inducible-Cas9 system.

INTRODUCTION

Tauopathies

More than 40 million people world-wide are currently affected by tauopathies– a class of neurodegenerative diseases in which intracellular aggregates of the microtubule-associated protein tau (*MAPT* gene, tau protein) are a major pathological characteristic (see: https://alz.org/global). Tau is a microtubule-associated protein that stabilizes microtubules and mediates axonal transport (Weingarten, 1975; Rodríguez-Martín et al., 2013). In pathology, tau aggregates into paired helical filaments and neurofibrillary tangles (Kosik et al., 1986). This pathology characterizes all tauopathies, including Alzheimer's Disease (AD), progressive supranuclear palsy (PSP), corticobasal degeneration (CBD), and frontotemporal dementia with parkinsonism linked to chromosome 17 (FTDP-17) (Iqbal et al., 1986; Warren et al., 2005). In each of these conditions, tau pathology is thought to contribute to cell death in the brain (Wang and Mandelkow, 2016), but the mechanisms by which tau protein forms toxic aggregates and facilitates neurodegeneration are still under investigation. Hyperphosphorylation (Grundke-Iqbal et al., 1986) and decreased degradation of tau (Chesser et al., 2013) have been hypothesized to promote its aggregation and thereby contribute to disease. The autophagy-lysosome system has been shown to play a role in the normal clearance of tau protein and impaired autophagy is a common characteristic in post-mortem brain tissue attained from tauopathy patients (Piras et al., 2016). Therefore, this study investigates the possibility that tau protein forms toxic aggregates as a result of impairments in the autophagy pathway.

Tau protein in physiology and pathology

Tau is a microtubule-associated protein that promotes the stability of

microtubules by binding to and increasing the rate of microtubule polymerization and decreasing the frequency of catastrophe, a process in which microtubules spontaneously begin depolymerizing (Weingarten, 1975). When microtubule catastrophe occurs, depolymerization proceeds at a slower rate as a result of tau-mediated stabilization (Drechsel et al., 1992). Human tau is encoded by the *MAPT* gene, and is normally localized in the axons of mature neurons (Hirokawa et al., 1996). Here, it regulates axonal transport by competing with the motor proteins kinesin and dynein for microtubule binding (Binder et al., 1985; Stamer et al., 2002). Because kinesin and dynein regulate anterograde and retrograde axonal transport, respectively (Vale, 2003), the competition between tau and these motor proteins provides cells with a homeostatic mechanism by which the rate and direction of microtubule-mediated axonal transport can be altered according to cellular needs (Dixit et al., 2008). The ability of tau to perform these physiological functions is affected by its degree of phosphorylation, as phosphorylated forms of tau have a lower affinity for microtubules and sequester non-phosphorylated forms of tau (Lindwall and Cole, 1984). Hyperphosphorylation therefore promotes toxic tau aggregation (Alonso et al., 1994). However, hyperphosphorylation alone is not sufficient to induce aggregation, suggesting that tau only forms aggregates when hyperphosphorylation occurs in conjunction with other pathology-promoting factors (Wang and Mandelkow, 2016).

Autophagy and the Ubiquitin-Proteasome System

Eukaryotic cells have two primary homeostatic pathways that regulate protein turnover: the ubiquitin-proteasome system (UPS) and the autophagy-lysosome system.

The UPS is responsible for targeting small cytoplasmic proteins for proteolysis via ubiquitination-mediated targeting to the proteasome, which contains enzymes that unfold and degrade proteins (Voges et al., 1999).

Autophagy is a conserved cellular homeostasis pathway that is responsible for the normal turnover of damaged organelles, misfolded proteins, and protein aggregates, as well as for nutrient retrieval during starvation (Levine and Kroemer, 2008). In autophagy, cytoplasmic cargo is sequestered within a double-membraned vesicle called an autophagosome. Autophagosomes are targeted to the lysosome, where their cargo is degraded (Levine and Kroemer, 2008). Formation of autophagosomes is facilitated by autophagy-related (Atg) proteins such as *Atg5* and *Atg7*, and also involves the conversion of microtubule-associated protein 1A/1B-light chain 3 (LC3) from soluble LC3-I to autophagosome-membrane-associated LC3-II. (Mizushima and Klionsky, 2007). Conditional knockout of either *Atg5* or *Atg7* in mouse nervous tissue results in progressive neurodegeneration (Hara et al., 2006; Komatsu et al., 2006). Likewise, deficiencies in autophagy are apparent in several age-related neurodegenerative diseases, and these impairments are associated with the onset of protein aggregation that is believed to be neurotoxic (Sarkar et al., 2014). This association suggests that impairments in autophagy may be causative of the protein aggregation that contributes to neurodegeneration, and that rescue of these impairments may have rich therapeutic potential.

Approaches to modulation of autophagy

Regulation of the autophagy pathway presents a multitude of confounding variables, including effects on cellular stress, viability, and disruption of normal homeostasis (Klionsky et al., 2016). Pharmacological control of autophagy requires manipulation of upstream signaling pathways, including the inhibitory mTOR pathway, the stimulatory PI3K/AKT signaling pathway, or the stimulatory AMPK pathway (Heras-Sondoval et al., 2014), which has potential to cause off-target effects that threaten to confound autophagy-based interpretations. For example, inhibition of the mTOR complex by torin1 results in up to a 50% decrease in protein synthesis (Thoreen and Sabitini, 2009). Take also the small molecule 3-methyladenine (3-MA), which has been reported to inhibit protein degradation through the autophagy pathway via suppression of class III PI3K signaling (Seglen and Gordon, 1982; Petiot et al., 2000), and has subsequently been used as a canonical inhibitor of autophagy in several studies (Takatsuka et al., 2004; Stroikin et al., 2004; Hirosako et al., 2004). 3-MA has recently been demonstrated to exert both an inhibitory and stimulatory effect on autophagy via persistent inhibition of class III PI3K and transient inhibition of class I PI3K, respectively (Wu et al., 2010). 3-MA also has several known non-autophagic effects, including inhibition of endocytosis (Mizushima, 2004), illustrating the volatility of pharmacological modulation of autophagy.

As an alternative approach, genetic studies have facilitated extensive progress in understanding the role of autophagy in many cellular functions including embryonic development, stem cell differentiation, protein and organelle turnover, mitochondrial homeostasis (Suen et al., 2010), and the development of pathology. Autophagy has been

demonstrated to be essential for embryonic development as *Atg5*$^{-/-}$ and *Atg7*$^{-/-}$ mice are embryonic lethal (Tsukamoto et al., 2008; Kuma et al., 2004; Komatasu et al, 2005; Yue et al., 2003). Autophagy has also been shown to be essential for iPSC reprogramming (Wu et al., 2015; Ma et al., 2015), and for the maintenance of stemness in muscle stem cells (Garcia-Prat et al., 2016). Thus, systemic genetic deletion of essential autophagy genes in embryonic or developmental tissue prevents proper development and differentiation of stem cells and has made it difficult to develop mouse models of defective autophagy. However, conditional knockout of *Atg5* and *Atg7* in mouse neural, hepatic, cardiac and skeletal tissue produces sufficiently viable mice that later develop tissue-specific pathology (Komatsu et al., 2006; Komatsu et al., 2007; Hara et al., 2006; Nakai et al., 2007; Raben et al., 2008). These conditional knockout studies only facilitate the analysis of the role of autophagy in developmental processes and they likely do not replicate the age-dependent dysfunctions in autophagy associated with disease-relevant pathologies. In this study, we developed an inducible system that utilizes the RNA-guided Clustered Regularly Interspaced Short Palindromic Repeats/Cas9 (CRISPR/Cas9) technology to allow for easily programmable genetic interrogation of the autophagy pathway and bypasses potential developmental defects brought on by systemic genetic disruption of autophagy.

Mechanisms of tau protein clearance

Several studies have suggested that different forms of tau are preferentially degraded by either autophagy or the UPS in normal homeostasis in different model systems. For example, two studies showed that unmodified forms of tau have a lower propensity for aggregation and are typically cleared via the UPS whereas aggregation-

prone forms of tau, such as caspase-cleaved tau and phosphorylated tau species, are preferentially cleared through autophagy in mouse hippocampus and in an immortalized cortical neuronal cell line (Jo et al., 2014; Dolan and Johnson, 2010). Another study showed that treatment with chloroquine, which raises the pH of the lysosome and inhibits autophagic clearance, significantly slows the degradation of tau and resulted in the accumulation of multiple monomeric and oligomeric forms of tau in primary rat neurons (Krüger et al., 2012). In human neuroblastoma cells that overexpress 4R0N tau, chloroquine also significantly slowed down tau degradation, and promoted its accumulation (Hamano et al., 2008). Also, genetically increasing the activity of the mammalian target of rapamycin (mTOR) pathway, which normally inhibits autophagy, resulted in an increase in both total tau levels as well as an increase in the phospho-tau/total tau ratio in a mouse model of tauopathy (Caccamo et al., 2013). The breadth of evidence suggests that autophagy plays an important role in the turnover of tau in both normal physiology and pathology, but the physiological mechanism of tau clearance has yet to be explored in human neurons.

RESULTS

Induction of autophagy results in a decrease in phospho-tau levels in hiPSC-derived differentiated neural stem cells.

In order to determine the mechanisms by which tau protein is cleared in human neurons, we first sought to inhibit autophagic flux by treating human induced pluripotent stem cell (hiPSC) derived differentiated neural stem cells (dNSCs) with chloroquine, which inhibits autolysosomal cargo degradation by raising the pH of the lysosome (Kovacs and Seglen, 1982). However, chloroquine was toxic at timepoints of 24 hours and longer (data not shown), preventing clear analysis of turnover or accumulation of tau, which is a long-lived cytoplasmic protein (Yamada et al., 2014).

Therefore, we instead tested the effects of known activators of autophagy on the levels of tau and phosphorylated forms of tau (phospho-tau). We found that dNSCs treated with the autophagy activators torin1 or trehalose for five days had significantly decreased levels of phospho-tau (Figure 1A & 1B) as well as a significant increase in the LC3-II/LC3-I ratio (Figure 1C), indicating an induction of autophagy. The levels of total tau protein were not significantly different after treatment with either compound, while the ratio of pSer396/404 tau (PHF1) to total tau did decrease significantly, indicating that treatment with these two compounds resulted in specific decreases in phospho-tau (Figure 1B).

Proteasomal inhibition induces autophagy and results in a decrease in both total tau and phospho-tau

In order to determine the role of the UPS on autophagy-mediated clearance of tau and phospho-tau, we treated dNSCs with the proteasomal inhibitor MG-132, which

completely inhibits 20S proteasomal activity in a dose-dependent manner within 24 hours (Figure 2A). When dNSCs were treated with MG-132 for 48 hours, significant decreases in phospho-tau and total tau were observed, but the ratio of phospho-tau to total tau did not change significantly (Figure 2B & 2D). These changes coincided with an induction of autophagy via a significant increase in the LC3-II/LC3-I ratio (Figure 2C). These data indicate that proteasomal inhibition activates autophagy and promotes the clearance of all forms of tau protein, suggesting that the autophagy pathway may serve as a backup for the UPS in physiological conditions, and its induction can promote clearance of both total tau and phsopho-tau.

Characterization of pCW-Cas9 system

In order to identify how autophagy and the UPS truly regulate the clearance of total and phospho-tau, we set out to establish a system that would allow us to disrupt autophagy in an efficient and inducible fashion. Using an inducible-knockout model is the recommended method for studying autophagy (Klionsky et al., 2016). We reasoned that this would also allow us to avoid disrupting cellular homeostasis during hiPSC development and differentiation into NSCs, as well as NSC growth and differentiation into dNSCs–an expected downfall of non-inducible systems. Thus, we set out to generate an inducible CRISPR/Cas9-based system that would facilitate straightforward interrogation into genotype-phenotype relationships in post-mitotic cells such as neurons. The CRISPR/Cas9 system facilitates easily programmable genetic perturbation that can provide high-throughput and efficient insight into gene function (Shalem et al., 2014; Wang & Wei et al., 2014; Mandegar et al., 2016; Dahlman et al., 2015). We designed a two-construct system in which a single guide RNA (sgRNA) and

doxycycline-inducible Cas9 would be separately integrated (Figure 3A & 3B). In this way, a clonal cell line could be generated in which the doxycyline-dependent Cas9-expressing construct (pCW-Cas9-Blast) is stably integrated, and then differentiated into NSCs. As NSCs, lentiviral transduction of the lentiGuide-Puro construct would allow for programmable and inducible knockout of target genes at any stage of differentiation or maturation of NSC-derived cell types (Sanjana et al., 2014).

In order to characterize this system, we first generated a polyclonal population of pCW-Cas9-Blast NSCs and treated them with doxycyline for 3 days to induce Cas9 expression (Figure 4A). Strikingly, later passages of any polyclonal population of pCW-Cas9 NSCs began to grow more slowly in the presence of blasticidin (data not shown), and ultimately lost blasticidin resistance suggesting that the NSCs had silenced the promoter used to drive the blasticidin resistance gene. Not surprisingly, these later passages of pCW-Cas9 NSCs also could not be induced to express Cas9 (Figure 4C). dNSCs grown from a later passage of pCW-Cas9 NSCs that were also transduced with sgRNAs targeting *p62* could not be induced to express Cas9, and did not disrupt expression of *p62* (Figure 4B). This loss of blasticidin resistance was observed following at least three viral transductions and in multiple iPSC-derived NSC lines with the same outcome: after blasticidin selection and with constant blasticidin selection pressure, and within 1-3 passages after viral transduction, NSC proliferation decreased (data not shown) and inducibility of Cas9 was lost. This passage-dependent decrease in blasticidin resistance and in inducibility was not observed in HEK 293FT cells, suggesting that loss of resistance was due to factors associated with human NSCs, not all human cell types (e.g. HEK 293FT cells; Figure 4D).

Characterization of 3G-iCas9 system

The previous data suggested that the pCW-Cas9 construct likely underwent targeted silencing in our NSCs. We reasoned that the silenced factor was likely the PGK-1 promoter, which drives expression of the rtTA element and the blasticidin resistance gene. Culturing of NSCs containing the lentiGuide-Puro construct in puromycin did not result in stunted growth as a function of passage, suggesting that the EF1α promoter driving puromycin resistance was not subjected to the same targeted silencing (data not shown). Therefore, we sought to re-engineer the inducible Cas9 system so that it is (1) reliant on the EF1α promoter and thus resistant to targeted silencing and (2) easily screened for a successful response to doxycyline. The newly designed three-construct system (3G-iCas9) allows for doxycyline-dependent co-expression of Cas9 and EGFP (Figure 5A & 5C), facilitating screening for successful inducibility by microscopy (Figure 5C), flow cytometry (Figure 5D), or immunoblotting (Figure 5C).

To characterize the 3G-iCas9 system, we transduced HEK 293FT cells with the 3G-iCas9 constructs and administered doxycyline for 7 days, which resulted in robust Cas9 and EGFP expression even though the cells were not selected or sorted for integration of both constructs (Figure 5C).

Next, NSCs were transduced with the 3G-iCas9 construct and then selected in blasticidin. 3G-iCas9 NSCs were induced for 3 days and FACS sorted for EGFP expression and a naïve NSC cell-surface signature (Yuan et al., 2011). These sorted, EGFP+ NSCs were expanded further for several passages, then analyzed for inducibility by flow cytometry (Figure 6C). Interestingly, administration of doxycyline for 3 days

resulted in fewer EGFP positive cells in the sorted population than in the unsorted population (Figure 5D), indicating a loss of inducibility in all but ~14% of 3G-iCas9 NSCs (Figure 6C). For further characterization of the 3G-iCas9 system, we analyzed an unsorted population of 3G-iCas9 NSCs by immunofluorescence, which showed that administration of doxycyline for 7 days can induce robust Cas9 and EGFP expression (Figure 6A). However, the Cas9 signal was not localized to the nucleus, which if consistent, would preclude Cas9 from generating double-stranded DNA breaks.

To quickly test if the 3G-iCas9 system functions to generate double-stranded breaks, we induced Cas9 in HEK 293FT cells that were transiently transfected with various highly validated constructs containing sgRNAs targeting multiple loci in the *MAPT* gene. Three days after transfection in the presence of doxycycline (Cas9 activation), only ~12% of induced cells generated editing events at the target locus (Figure 6B, *pCR blunt + rs242557*). However, cells that were transfected with the px458 plasmid, which expresses Cas9 and the same sgRNA, successfully underwent editing in the target sequence at an efficiency of 98% (Figure 6B). Taken together, these data demonstrate that 3G-iCas9 system currently lacks practical utility and would require modification and further characterization prior to its use in functional genetic screens.

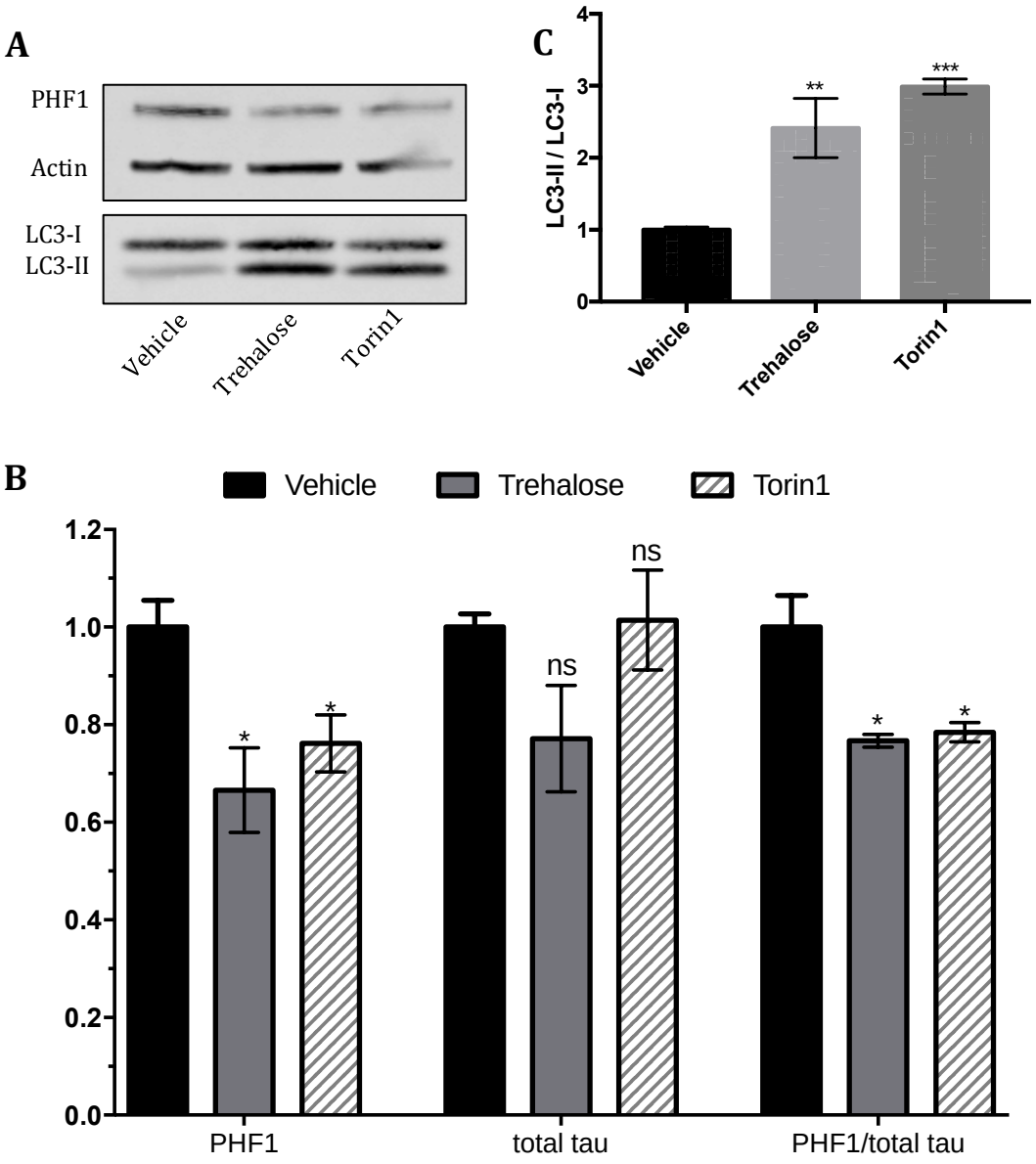

Figure 1. Induction of autophagy results in a decrease in phospho-tau levels. dNSCs were treated with 10uM Torin1 or 100mM trehalose for 5 days. **(A–C)** Western blot analysis demonstrates both autophagic induction via conversion of LC3-I to LC3-II and a decrease in p-Ser396/404 tau (PHF1) in response to treatments with each compound. **(B)** Densitometric quantification demonstrating that total tau protein, as well as the ratio of pSer396/404 to total tau do not significantly change in response to treatment with autophagic inducers. Torin1, n=5; Trehalose, n=3. *p<0.05, **p<0.01, ***p<0.001.

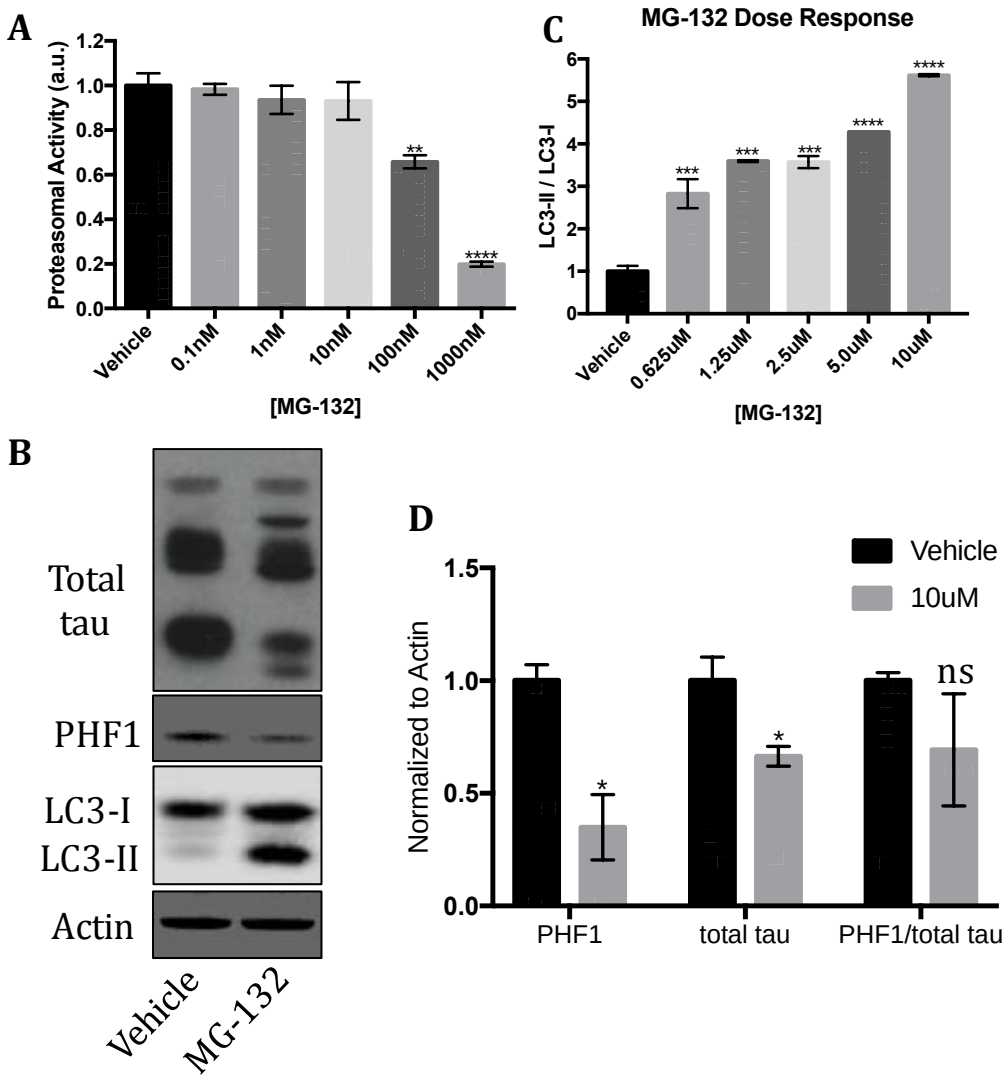

Figure 2. Proteasomal inhibition induces autophagy and results in a decrease in both total tau and phospho-tau. **(A)** 20S Proteasome activity assay demonstrates a dose-dependent decrease in proteasomal activity after treatment with MG-132 for 24 hours. **(B-D)** dNSCs were treated with up to 10uM MG-132 for 48 hours then analyzed by western blot. **(C)** Densitometric quantification of ratio of LC3-II to LC3-I. **(D)** Densitometric quantification of total tau (all bands shown) and p-Ser396/404 tau (PHF1). *p<0.05, **p<0.01, ***p<0.001, ****p<0.0001, ns = not significant (n=2 sets of treatments, each in duplicate).

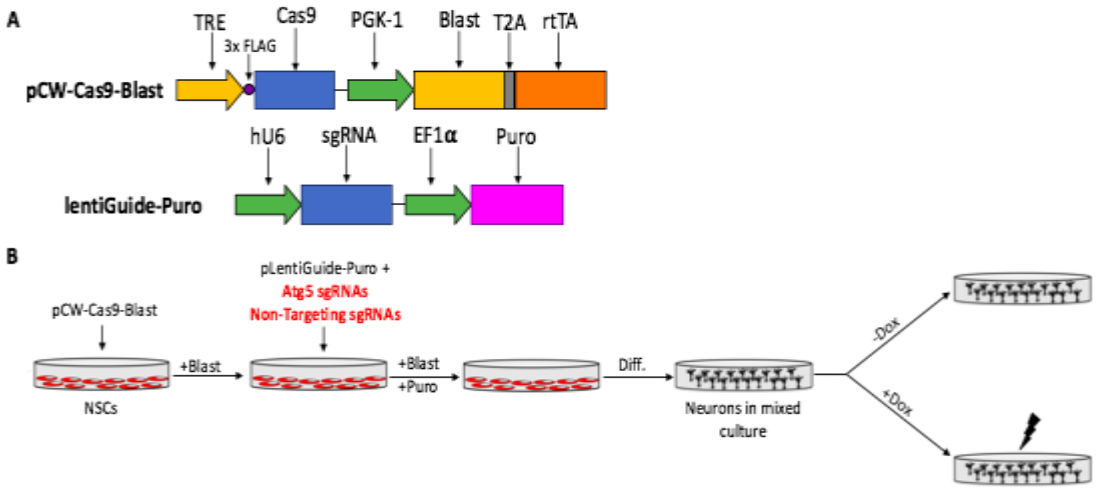

Figure 3. Design of pCW-Cas9 system. (A) In the pCW-Cas9-Blast construct, expression of Cas9 was controlled by the doxycycline-dependent TRE promoter, whereas the tetracycline-transactivator element (rtTA) and blasticidin resistance genes were controlled by the constitutively active PGK-1 promoter. Doxycycline associates with rtTA to induce transcription of the TRE promoter. Expression of the sgRNA and puromycin resistance genes on the lentiGuide-Puro construct were controlled by the constitutively active human U6 and EF1α promoters, respectively. **(B)** Schematic of cell culture process. Neural stem cells (NSCs) were transduced with the pCW-Cas9-Blast lentivirus then selected in blasticidin. Cells were then transduced with lentiGuide-Puro carrying one of three single guide RNAs (sgRNAs), then puromycin-selected before differentiation and subsequent induction of Cas9 to disrupt target genes.

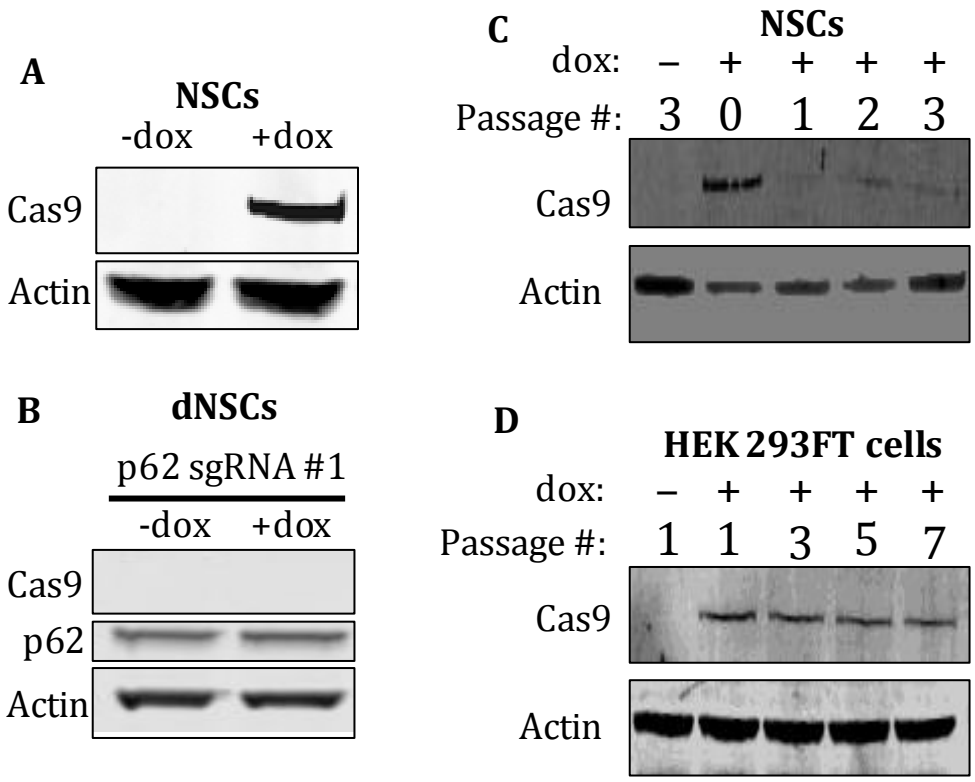

Figure 4. Characterization of pCW-Cas9 system. (A) NSCs transduced with pCW-Cas9-Blast and selected in blasticidin were administered doxycyline (dox) for 3 days and analyzed for Cas9 expression by western blot. **(B)** pCW-Cas9-Blast NSCs were further transduced with lentiGuide-Puro containing an sgRNA targeting p62, differentiated into dNSCs for 6 weeks, and then administered dox for 3 days. **(C)** pCW-Cas9-Blast NSCs were administered dox for 7 days at several different passages after transduction. **(D)** HEK 293FT cells were transduced with pCW-Cas9-Blast and treated with dox for 7 days at several different passages to induce expression of Cas9.

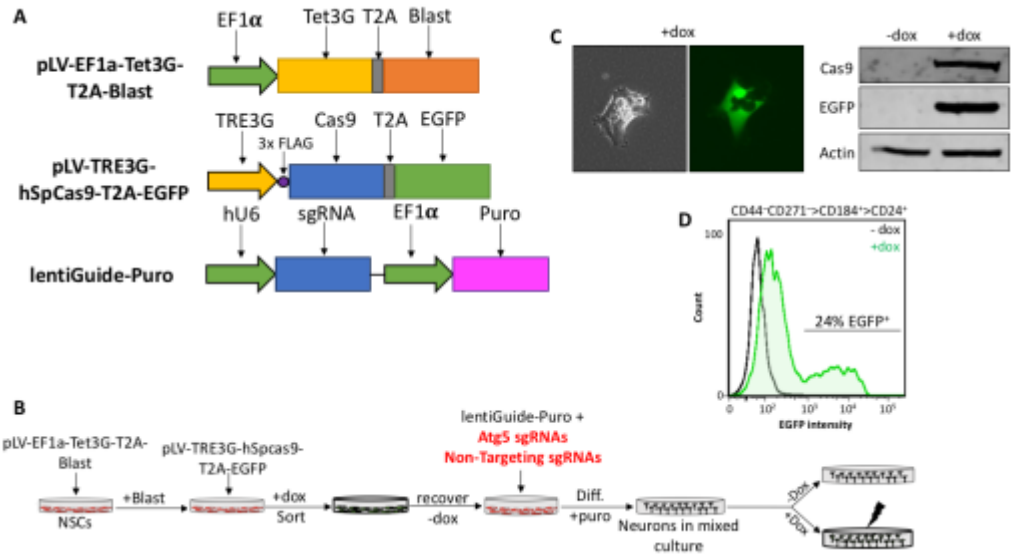

Figure 5. Design and basic characterization of third-generation inducible-Cas9 (3G-iCas9) system. (A) Schematic of 3G-iCas9 system. Expression of Cas9 was controlled by the doxycycline-dependent TRE3G promoter, whereas the tetracycline-transactivator element (Tet3G) and blasticidin resistance genes were controlled by the constitutively active EF1α promoter. Expression of the sgRNA and puromycin resistance genes on the lentiGuide-Puro construct were controlled by the constitutively active human U6 and EF1α promoters, respectively. **(B)** Cell culture schematic. NSCs were transduced with 3G lentiviruses, selected in blasticidin, and FACS sorted for EGFP expression after 3 days of doxycyline treatment. Then NSCs were transduced with lentiGuide-Puro containing sgRNAs and selected in puromycin prior to differentiation into neuronal mixed cultures, then induced to disrupt target gene function. **(C)** Fluorescence microscopy and western blot demonstrate EGFP and Cas9 expression after induction. **(D)** Transduced NSCs were sorted by FACS for EGFP expression and a naïve NSC signature ($CD44^{-}/CD271^{-}>CD184^{+}>CD24^{+}$).

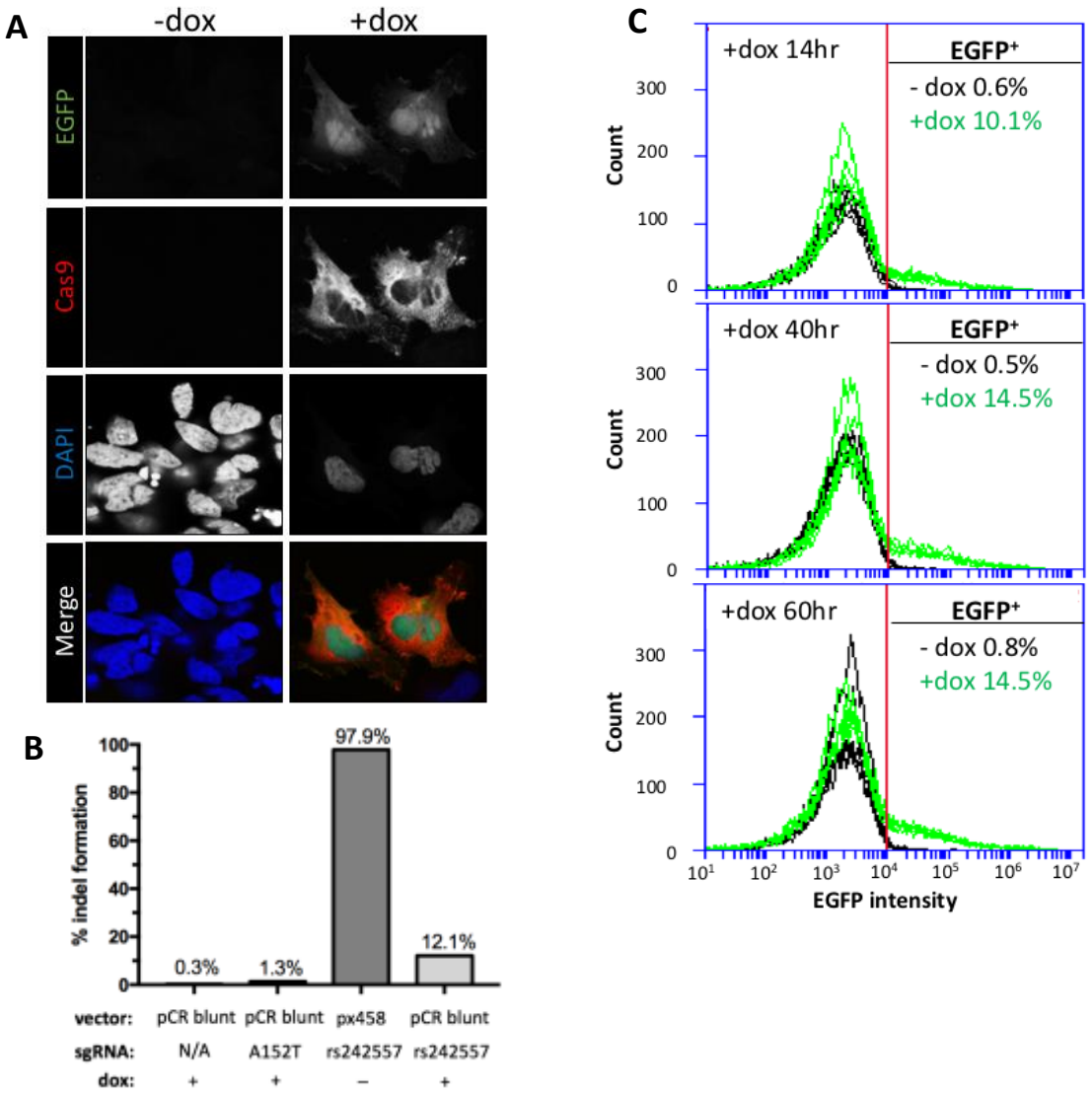

Figure 6. Functional characterization of 3G-iCas9 system in NSCs and HEK 293FT cells. (A) Immunofluorescence demonstrating EGFP and Cas9 expression upon doxycyline-mediated induction, but a lack of nuclear Cas9 localization. **(B)** TIDE analysis of formation of insertions and deletions (indels) upon transfection of sorted 3G-iCas9 HEK 293FT cells with vectors carrying various validated sgRNAs. px458 as positive control, pCR blunt vector without an sgRNA and pCR blunt + A152T sgRNAs as negative controls (n=1). **(C)** Flow cytometry demonstrating EGFP expression in sorted 3G-iCas9 NSCs after 14, 40, and 60 hours of treatment with doxycyline.

DISCUSSION

Induction of autophagy results in a decrease in phospho-tau levels in hiPSC-derived differentiated neural stem cells

In this study, we have demonstrated that autophagic induction with the compounds torin1 and trehalose is associated with a decrease in phospho-tau (Figure 1) in human dNSCs. Torin1 is an inhibitor of mTORC1, a kinase that has been shown to promote tau phosphorylation via GSK3β activity (Caccamo et al., 2013). Because the amount of total tau does not significantly decrease in response to treatment with torin1, we wanted to test if the decrease in phospho-tau was due to a decrease in mTOR-mediated phosphorylation of tau, or due to increased turnover of tau due to induction of autophagy. So we treated cells with the compound trehalose, which enhances autophagy through an mTOR-independent mechanism (Sarkar et al., 2007) and has been shown to promote clearance of protein aggregates in neural tissue, including tau (Krüger et al., 2012; Schaeffer et al., 2012), α-synuclein (Casarejos et al., 2011), and mutant huntingtin (Sarkar et al., 2007). Furthermore, trehalose was recently shown to ameliorate neurodegenerative symptoms in an iPSC-derived neuronal model of progranulin haploinsufficincy via an induction of autophagy (Holler et al., 2016). Trehalose also induced autophagy in our system (Figure 1C), and promoted clearance of phospho-tau (Figure 1A & 1B). Thus, we have shown that induction of autophagy by two independent mechanisms can similarly promote a decrease in phospho-tau. However, further characterization of the effects of these compounds still needs to be performed, including an assessment of the effect(s) on other phospho-tau epitopes and downstream mTOR targets, including GSK3β.

Proteasomal inhibition induces autophagy and results in a decrease in both total tau and phospho-tau

In this study, we characterized the effects of inhibition of the 20S proteasome on autophagy activity and phospho-tau stasis, finding that when the proteasome is inhibited for 48 hours, autophagy is strongly induced in human dNSCs (Figures 2C). This induction of autophagy coincides with a decrease in phospho-tau, but also causes a decrease in total tau without affecting the phospho-tau:total tau ratio (Figure 2D). These data are in concert with some current literature (Krüger et al., 2012; Lei et al., 2015), which have shown that proteasomal inhibition in primary rat cortical neurons results in an induction of autophagy and a coincident decrease in both phospho- and total tau. However, these results conflict with other reports that proteasomal inhibition does not induce autophagy in primary rat cortical neurons (Fan et al., 2016). Taken together, our data suggest that the proteasome, not autophagy, is responsible for the turnover of non-phosphorylated forms of monomeric tau in normal physiology, as induction of autophagy without coincident proteasomal inhibition did not affect these forms of tau (Figure 1B). Our results also suggest that autophagy can serve as a sufficient backup system for the cell when proteasomal activity is disrupted.

Characterization of pCW-Cas9 system

As previously described, genetic perturbation of autophagy requires careful consideration because autophagy is critical during cellular development and stem cell differentiation, as well as in normal homeostasis. Thus, the need for an inducible system of genetic disruption has emerged, especially in cellular models such as hiPSC-derived neurons, in which heterogeneity due to genetic differences during development and

differentiation would likely confound any obtained results. siRNA and shRNA-mediated knockdown of essential autophagy genes has successfully been performed previously to perturb autophagy (Lv et al., 2014; Wang & Li et al., 2014). This strategy has been shown to be reliable and can also be inducible (Matsushita et al., 2013), but does not produce complete knockdown in most systems. We reasoned that a CRISPR/Cas9-based strategy could generate more complete, simple, and programmable perturbation that could be re-purposed for larger genetic screens in hiPSC-derived neurons, however, we first sought to understand the efficiency of these tools in relevant cell types.

The pCW-Cas9 system was previously used for genome-wide genetic screens in mammalian cells via doxycyline-inducible genetic perturbations (Wang & Wei et al., 2014). We modified the construct so that it would contain a gene driving blasticidin resistance rather than puromycin resistance, and would thus be compatible with the lentiGuide-Puro system (Sanjana et al., 2014). We found that the pCW-Cas9 construct likely underwent targeted silencing in our NSCs, and thus failed to maintain doxycyline-inducible Cas9 expression over time (Figure 4B & 4C). Because NSCs halted proliferation in the persistent presence of blasticidin, we reasoned that the silencing was likely of the PGK-1 promoter driving blasticidin resistance in pCW-Cas9-Blast. This promoter has been shown to produce ubiquitous transgene expression in primary rat neuronal and astrocyte cultures (Qin et al., 2010), but very little transgene expression in lung epithelial tissue (Xu et al., 2001). This suggests that the PGK-1 promoter may have cell-type specific activity, and it is possible that our neural stem cells silence this promoter efficiently.

Characterization of 3G-iCas9 system

The 3G-iCas9 system (Figure 5) contains optimized doxycyline-inducible elements (TRE3G and Tet3G) as well as blasticidin resistance driven by the EF1α promoter, which has been shown to promote high transgene expression in neurons (Tsuchiya et al., 2002) and in stem cells (Hong et al., 2007), which would facilitate the use of the system in both neurons and iPSCs. We also saw that NSCs tended to proliferate more readily in puromycin (resistance driven by the EF1α promoter in lentiGuide-Puro) than in blasticidin (resistance driven by the PGK-1 promoter in pCW-Cas9). Thus, the 3G system was designed to be more easily screened and characterized, as well as be more reliable and efficient in our cells than the pCW-Cas9 system.

We characterized the 3G-iCas9 system and found that it could be induced to express both EGFP and Cas9 upon treatment with doxycyline (Figure 5C). We also found that in both HEK 293FT cells and NSCs, Cas9 and EGFP were not expressed in the absence of doxycyline, indicating that the TRE3G promoter was not leaky–an essential quality control to ensure reliability for small-scale and larger-scale genetic screens (Figure 5C). After basic characterization, we later found that cleavage efficiency of the 3G-iCas9 was very low relative to transiently transfected Cas9 + sgRNA via px458 (Figure 6B). This may be related to a difference in the ratio of Cas9 to sgRNA in each cell, as at least one previous study has shown that when more Cas9 is expressed than sgRNA, cleavage efficiency is decreased (Li et al., 2013). It is also possible that transient transfection results in more robust Cas9 expression, and thus produces more on-target cleavages (Hsu et al., 2013) than doxycyline-induced Cas9 expression alongside transiently transfected sgRNA. However, we observed high Cas9 expression

in the presence of doxycyline by immunofluorescence and western blot (Figures 5C and 6A). We also observed that only ~14% of NSCs could be induced to express Cas9 and EGFP upon induction, even though they had previously been sorted for strong EGFP expression (Figures 6D & 5D). These data suggest that we may once again have targeted silencing of the 3G-iCas9 system as a result of continued passaging, even though the cells were also sorted for a naïve NSC signature (Figure 5D). It is also possible that the TRE3G promoter was specifically silenced, and we did not notice because of the lack of a selection cassette in that construct. Another observation was the localization of induced Cas9 primarily to the cytoplasm rather than the nucleus (Figure 6A). The Cas9 expressed by the 3G-iCas9 construct contains three nuclear localization sequences (NLS) fused to the N-terminus of the protein, and has been previously been shown to enter the nucleus and generate double-stranded breaks (Cong et al., 2013). Therefore, it would be expected that Cas9 would localize to the nucleus to a greater extent than it did.

Concluding remarks and future directions

In summary, this study has characterized the effects of autophagic induction and proteasomal inhibition on tau and phospho-tau clearance in human induced pluripotent stem cell-derived neurons. We would next like to test the hypothesis that autophagy mediates phospho-tau clearance by generating autophagy-deficient neurons. Because the inducible-Cas9 system has been troubling to optimize, it may be simpler and more efficient to use shRNAs targeting essential autophagy genes such as *Atg5*, *Atg7*, and *Beclin1*, or express a dominant-negative form of *Atg5*, which has been shown to efficiently knockdown autophagy (Pyo et al., 2005). Studying the effects of autophagic and proteasomal inducers and inhibitors in autophagy-deficient neurons

would provide greater clarity as to the role of autophagy in the normal turnover of tau and phospho-tau. We would specifically like to see if autophagy-deficient neurons treated with torin1 and trehalose still reduce phospho-tau regardless of autophagic ability. If this were the case, then this would support a hypothesis that phospho-tau is either being dephosphorylated (or is undergoing less nascent phosphorylation) or cleared through another pathway such as the UPS. If the noted decrease in phospho-tau is dependent on intact autophagic clearance, then the likely interpretation is that autophagy is an essential mediator of phospho-tau degradation. Future studies might further interrogate which specific forms of tau (isorforms, caspase-cleaved, etc.) accumulate in autophagy-deficient neurons, and in those that are also UPS-limited.

As for the inducible-Cas9 system, our data suggest that mindful consideration of the methodology and approach must be employed for generating a system that can be used for genome-wide and small-scale genetic screens in human iPSC-derived cell types. An inducible CRISPR interference (CRISPRi) system has recently been shown to generate efficient, tunable, and reversible disruption of target genes via sgRNA-mediated transcriptional repression (Mandegar et al., 2016). A screen executed by transcriptional repression as opposed to induced loss-of-function at the genomic level would avoid complications brought on by incomplete loss-of-function and potential gain-of-functions generated by random mutagenesis during DNA repair by non-homologous end-joining. This alternative approach would also avoid complications that may arise from inducing DNA damage in post-mitotic cells such as neurons, in which DNA repair mechanisms are not fully understood. However, the CRISPRi system is less optimized than the use of traditional sgRNA-guided Cas9 endonuclease,

and thus using this system for genome-wide screens would require significant optimization and characterization prior to its application in the desired cell types. Lastly, considering the troubles we have had in reliably expressing lentiviral constructs, it may also be necessary to systematically characterize different promoter sequences delivered by lentivirus into our NSCs and dNSCs to determine an optimal system for all future studies.

MATERIALS AND METHODS

Plasmid constructs

The pCW-Cas9-Blast plasmid was modified from pCW-Cas9, a gift from Eric Lander and David Sabitini (Addgene plasmid # 50661), by replacing the puromycin resistance gene with a blasticidin resistance gene. pSpCas9(BB)-2A-GFP (PX458) and lentiGuide-Puro were gifts from Feng Zhang (Addgene plasmids #48138 and #52963, respectively). pLV-EF1a-Tet3G-T2A-Blast and pLV-TRE3G-hSpCas9-T2A-EGFP were designed using VectorBuilder.com and synthesized by Cyagen. For lentiviral packaging, psPAX2 and pMD2.G were gifts from Didier Trono (Addgene plasmids #12260 and #12259, respectively). The pCR™-Blunt vector was purchased from Thermo Scientific (#K270040).

HEK 293FT cell culture

Human Embryonic Kidney (HEK) cell line 293FT (Thermo Scientific) was maintained in Dubecco's Modified Eagle Medium (4.5 g/L glucose), supplemented with 2mM L-Glutamine (Gibco), 10% FBS (Corning), and 100U/mL penicillin-streptomycin (Gibco), at 37°C with 5% CO_2. Upon reaching 80-90% confluency, cells were dissociated using 0.25% trypsin-EDTA (Gibco) then passaged into uncoated plates at a ratio of 1:4. pCW-Cas9 and 3G-iCas9 HEK 293FT cells were cultured in the presence of blasticidin (Corning; 10μg/mL) with or without puromycin (Invitrogen; 5μg/mL).

NSC and differentiated NSC culture

NSCs were generated from iPSCs using previously published protocols (Israel et al., 2012 and Yuan et al., 2011). NSCs were maintained in DMEM/F12 medium (Thermo) supplemented with B-27 and N-2 (Life Technologies), as well as penicillin-streptomycin (100U/mL) and FGF (EMD Millipore, 20ng/mL). Upon reaching ~80-

90% confluency, NSCs were dissociated with Accutase (Innovative Cell Technologies) then passaged at a 1:3 ratio onto poly-L-ornithine (0.002% in water) and laminin (5µg/mL in DPBS) coated plates. NSCs were differentiated by FGF withdrawal and cultured for at least three weeks, defining them as neuronal mixed cultures (differentiated NSCs or dNSCs), prior to experimental manipulations.

pCW-Cas9 and 3G-iCas9 dNSCs were cultured in blasticidin (1-5µg/mL), and if applicable, puromycin (1µg/mL), unless otherwise stated.

Transfections and lentiviral transductions

293FT cells were seeded into poly-L-ornithine coated 6-well plates (Corning) one day prior to transfection at a density of 10^6 cells per well. Cells were transfected using LipoD293™ In Vitro Transfection Reagent (SignaGen) following the manufacturer's recommended protocol (e.g. 3:1 µL LipoD293: µg DNA). Each well of a 6-well plate was transfected with 2µg of total plasmid, including 750ng of psPAX2 (Addgene plasmid #12260) and 250ng pMD2.G (Addgene #12259), then the media was replaced after 14-18 hours. Two days later, media was collected and filtered through a 0.45µm PVDF filter then stored at -80°C.

For lentiviral transductions, 10^5 HEK 293FT cells or 10^6 NSCs were seeded per well of a 6-well plate with 1mL of virus-containing media at an unknown MOI (typical titers were $>10^6$ infectious units per ml from un-concentrated virus preparations, however virus was not routinely tittered). Virus-containing media was removed after 12-36 hours and replaced with fresh media.

BCA protein concentration assay

Protein concentration of lysates was measured using the Pierce BCA Protein Assay Kit (Thermo Scientific) according to the manufacturer's protocol and extrapolated from a standard curve generated from serial dilutions of BSA.

Immunoblotting

Prior to collection, cells were washed once with PBS and lysed with RIPA Buffer (50mM Tris, 150mM NaCl, 1mM EDTA, 1% Triton X, 0.25% deoxycholate) with 1mM Na_3VO_4, 5µM $ZnCl_2$, 100mM NaF, 1mM PMSF in isopropanol, and 1µM Pepstatin with protease inhibitors diluted in MilliQ water. Lysates were vortexed for 30 seconds, then cleared by centrifugation at 14,000 g for 20 minutes at 4°C. Supernatant was boiled at 100°C for 10 minutes in 1x SDS sample loading buffer (715mM β-Mercaptoethanol). For analysis, samples (2-20µg of protein) were separated on 4-12% Bis-Tris precast gels (Life Technologies, #WG1401) for 1 hour at 200V in 1x MES buffer, followed by transfer onto 0.2µm PVDF membranes at 40V for 2 hours at 4°C (BioRad, #162-0177). After transfer, membranes were blocked for 1 hour at room temperature in 5% milk in TBS-Tween, then incubated overnight in the indicated primary antibody diluted in TBS-Tween with 15mM sodium azide. Membranes were then washed for 10 minutes three times, then incubated in indicated secondary antibodies for 1 hour at room temperature. Membranes were then washed 5 times for 10 minutes in PBS then developed on the LI-COR Odyssey Imaging System.

Drug treatments

After 3-6 weeks of differentiation, dNSCs were treated in triplicate on 24-well plates or in duplicate on 12-well plates with 1-10µM torin1, 50-100mM Trehalose, or

0.1-1μM MG-132 for up to 5 days (see Table 3) alongside a 0.1% DMSO vehicle-treated population. After treatment, cells were imaged on a Zeiss Axio Vert A1 inverted microscope, cell supernatant was collected for LDH Cytotoxicity Assay, and cells were harvested for protein in either RIPA buffer for immunoblotting or MSD Tris Lysis Buffer (MSD, #R60TX-3) with protease and phosphatase inhibitors for ELISA.

Proteasome activity assay

The activity of 20S proteasomes was measured using the 20S Proteasome Assay Kit (Cayman #10008041). HEK 293FT cells were plated at a density of 10^5 cells per well onto a 96-well plate and treated in triplicate for 24 hours with 1:10 serial dilutions of MG-132 (0.1nM-1000nM). Fluorescence of the cleaved 20S specific substrate SUC-LLVY-AMC was measured on a plate reader (excitation = 360nm, emission = 480nm).

Lactate Dehydrogenase (LDH) cytotoxicity assay

After drug treatments, cell supernatant was collected to measure the toxicity of a given compound using the LDH-Cytotoxicity Colorimetric Assay Kit II (Biovision #K313). Assays were performed according to the manufacturer's protocol.

PCR and TIDE-seq analysis

Genomic DNA was extracted using QuickExtract™ DNA Extraction Solution (epicenter, #QE09050) according to the manufacturer's protocol. RNA was extracted using the SV Total RNA Isolation System (Promega, # Z3100). PCR amplification was run with indicated primer sets (see Table 4) using Phusion® High-Fidelity PCR Master Mix with HF Buffer (NEB, M0531S). Sanger sequencing of PCR products was performed by Eton Biosciences, and these sequences were deposited to TIDE (Brinkman et al., 2014), and analyzed for indel formation.

Immunofluorescence

Cells were cultured in Nunc™ Lab-Tek™ Chamber Slides (NUNC #177402). Cells were washed once with PBS then fixed with 4% paraformaldehyde at room temperature for 30 minutes. Fixed cells were then washed three times with PBS then blocked for one hour at room temperature in 5% BSA with 0.1% Triton-X. Cells were then incubated overnight at 4°C with gentle agitation in primary antibody diluted in 5% BSA without Triton-X. Then, cells were washed in PBS three times for 20 minutes each at room temperature with gentle agitation. Then, cells were incubated overnight in secondary antibody diluted in 5% BSA at 4°C with gentle agitation. Then cells were washed five times for 20 minutes with PBS at room temperature. The fourth wash included DAPI diluted in PBS. Coverslips were mounted onto slides using VECTASHIELD HardSet Antifade Mounting Medium (#H-1400) at room temperature for four hours in the dark, then overnight at 4°C. Slides were then imaged on a Zeiss confocal microscope.

FACS and flow cytometry

3G-iCas9 HEK 293FT cells and NSCs were induced with 10μg/mL doxycyline for 72 hours then sorted for GFP+ signal using the BD FACSAria Cell Sorter (BD Biosciences). Flow cytometry analysis was performed using the BD Accuri™ C6 Plus flow cytometer and analyzed with FlowJo Version7.6.1.

sgRNA design, sequences, and cloning into the lentiGuide-Puro plasmid

p62 sgRNA #1 (see Table 5) was obtained from the GeCKOv2 library (Shalem et al., 2014). sgRNA oligos (obtained from IDT) were phosphorylated, annealed and cloned into the lentiGuide-Puro backbone using a BsmBI ligation strategy. Competent

Stbl3 cells were then transformed with recombinant lentiGuide-Puro and cultured overnight on LB-Ampicillin plates. *MAPT* A152T (rs143624519) and rs242557 targeting sgRNAs were designed by Jordan Dizon. Briefly, the surrounding sequence was obtained from the UCSC genome assembly and deposited into the CRISPR tool on genome-engineering.org. sgRNAs were chosen for the target locus based on low off-target prediction. For the reported studies, the *MAPT* A152T sgRNA was used as a control, because it did not target the same region of the *MAPT* gene as rs242557.

Statistics and other software

For each bar graph represented, statistics were performed by either using a one-way ANOVA with Dunnet correction for multiple comparisons, or by two-tailed Student's t-test using GraphPad Prism 7. The data were presented as the mean ± SEM. Graphs were generated on Prism, and edited in Microsoft PowerPoint.

Table 1. Primary antibodies used for immunoblotting and immunofluorescence

Primary Antibodies				
Antibody	**Host Species**	**Manufacturer**	**Catalog #**	**Dilution**
Actin C4	M	EMD/Millipore	MAB1501	1:50,000
Cas9	M	CST	14697	1:1,000
FLAG	R	Sigma	F7425	1:1,000
EGFP	M	CST	2955S	1:1,000
Total tau	R	Sigma	T6402	1:1,000
PHF1 tau	M	Gift from Peter Davies		1:2,000
LC3-B	R	Novus Biologicals	NB100-2220	1:2,000

Table 2. Secondary antibodies used for immunoblotting

Secondary Antibodies			
Antibody	**Manufacturer**	**Catalog #**	**Dilution**
IRDye® 800CW Goat anti-Mouse IgG (H + L)	Li-Cor	925-32210	1:5000
IRDye® 800CW Goat anti-Rabbit IgG (H + L)	Li-Cor	925-32211	1:5000
IRDye® 680RD Goat anti-Mouse IgG (H + L)	Li-Cor	925-68070	1:5000
IRDye® 680RD Goat anti-Rabbit IgG (H + L)	Li-Cor	925-68071	1:5000
HRP Goat Anti-Rabbit IgG	Vector	PI-1000	1:5000
HRP Goat Anti-Mouse IgG	Vector	PI-9401	1:5000

Table 3. Reagents used for immunofluorescence

Reagent	Conjugation	Manufacturer	Catalog #	Dilution
Goat anti-Mouse IgG (H+L), Secondary antibody	Alexa Fluor® 568	Invitrogen	A-11004	1:2000
Goat anti-Rabbit IgG (H+L), Secondary antibody	Alexa Fluor® 568	Invitrogen	A-11011	1:2000
4′,6-Diamidine-2′-phenylindole dihydrochloride (DAPI)	N/A	Sigma	10236276001	1:5000

Table 4. Compounds used for modulating autophagy

Compound	Manufacturer	Catalog #
D-(+)-Trehalose Dihydrate	Sigma	T0167
Torin1	Sigma	475991
MG-132	EMD Millipore	474791

Table 5. sgRNA sequences

sgRNA	Sequence (5'→3')
p62 #1	ACGCTACACAAGTCGTAGTC
MAPT A152T	CGCCACCTTGACTCAAAACG
MAPT rs242557	AAAGCAGTTGGCTTCGCCCA

REFERENCES

Alonso, A.C., Zaidi, T., Grundke-Iqbal, I., Iqbal, K., 1994. Role of abnormally phosphorylated tau in the breakdown of microtubules in Alzheimer disease. Proceedings of the National Academy of Sciences of the United States of America 91, 5562–5566.

Binder, L., Frankfurter, A., Rebhun, L., 1985. The distribution of tau in the mammalian central nervous system. The Journal of Cell Biology 101, 1371–1378.

Caccamo, A., Magrì, A., Medina, D.X., Wisely, E.V., López-Aranda, M.F., Silva, A.J., Oddo, S., 2013. mTOR regulates tau phosphorylation and degradation: implications for Alzheimer's Disease and other tauopathies. Aging cell 12, 370–380.

Casarejos, M.J., Solano, R.M., Gómez, A., Perucho, J., de Yébenes, J.G., Mena, M.A., 2011. The accumulation of neurotoxic proteins, induced by proteasome inhibition, is reverted by trehalose, an enhancer of autophagy, in human neuroblastoma cells. Neurochemistry International 58, 512–520.

Chesser, A.S., Pritchard, S.M., Johnson, G.V.W., 2013. Tau Clearance Mechanisms and Their Possible Role in the Pathogenesis of Alzheimer Disease. Frontiers in Neurology 4, 122.

Cong, L., Ran, F.A., Cox, D., Lin, S., Barretto, R., Habib, N., Hsu, P.D., Wu, X., Jiang, W., Marraffini, L.A., Zhang, F., 2013. Multiplex Genome Engineering Using CRISPR/Cas Systems. Science 339, 819–823.

Dahlman, J.E., Abudayyeh, O.O., Joung, J., Gootenberg, J.S., Zhang, F., Konermann, S., 2015. Orthogonal gene knockout and activation with a catalytically active Cas9 nuclease. Nat Biotech 33, 1159–1161.

Dixit, R., Ross, J.L., Goldman, Y.E., Holzbaur, E.L.F., 2008. Differential Regulation of Dynein and Kinesin Motor Proteins by Tau. Science (New York, N.Y.) 319, 1086–1089.

Dolan, P.J., Johnson, G.V.W., 2010. A Caspase Cleaved Form of Tau Is Preferentially Degraded through the Autophagy Pathway. The Journal of Biological Chemistry 285, 21978–21987.

Drechsel, D.N., Hyman, A.A., Cobb, M.H., Kirschner, M.W., 1992. Modulation of the dynamic instability of tubulin assembly by the microtubule-associated protein tau. Molecular Biology of the Cell 3, 1141–1154.

Fan, W., Long, Y., Lai, Y., Wang, X., Chen, G., Zhu, B., 2016. NPAS4 Facilitates the Autophagic Clearance of Endogenous Tau in Rat Cortical Neurons. Journal of Molecular Neuroscience 58, 401–410.

García-Prat, L., Martínez-Vicente, M., Perdiguero, E., Ortet, L., Rodríguez-Ubreva, J., Rebollo, E., Ruiz-Bonilla, V., Gutarra, S., Ballestar, E., Serrano, A.L., Sandri, M., Muñoz-Cánoves, P., 2016. Autophagy maintains stemness by preventing senescence. Nature 529, 37–42.

Goedert, M., Jakes, R., 1990. Expression of separate isoforms of human tau protein: correlation with the tau pattern in brain and effects on tubulin polymerization. The EMBO Journal 9, 4225–4230.

Grundke-Iqbal, I., Iqbal, K., 1999. Tau Pathology Generated by Overexpression of Tau. The American Journal of Pathology 155, 1781–1785.

Hamano, T., Gendron, T.F., Causevic, E., Yen, S.-H., Lin, W.-L., Isidoro, C., DeTure, M., Ko, L., 2008. Autophagic-lysosomal perturbation enhances tau aggregation in transfectants with induced wild-type tau expression. European Journal of Neuroscience 27, 1119–1130.

Hara, T., Nakamura, K., Matsui, M., Yamamoto, A., Nakahara, Y., Suzuki-Migishima, R., Yokoyama, M., Mishima, K., Saito, I., Okano, H., Mizushima, N., 2006. Suppression of basal autophagy in neural cells causes neurodegenerative disease in mice. Nature 441, 885–889.

Heras-Sandoval, D., Pérez-Rojas, J.M., Hernández-Damián, J., Pedraza-Chaverri, J., 2014. The role of PI3K/AKT/mTOR pathway in the modulation of autophagy and the clearance of protein aggregates in neurodegeneration. Cellular Signalling 26, 2694–2701.

Hirokawa, N., Kanai, Y., 1996. Selective stabilization of tau in axons and microtubule-associated protein 2C in cell bodies and dendrites contributes to polarized localization of cytoskeletal proteins in mature neurons. The Journal of Cell Biology 132, 667–679.

Hirosako, K., Imasato, H., Hirota, Y., Kuronita, T., Masuyama, N., Nishioka, M., Umeda, A., Fujita, H., Himeno, M., Tanaka, Y., 2004. 3-Methyladenine specifically inhibits retrograde transport of cation-independent mannose 6-phosphate/insulin-like growth factor II receptor from the early endosome to the TGN. Biochemical and Biophysical Research Communications 316, 845–852.

Holler, C.J., Taylor, G., McEachin, Z.T., Deng, Q., Watkins, W.J., Hudson, K., Easley, C.A., Hu, W.T., Hales, C.M., Rossoll, W., Bassell, G.J., Kukar, T., 2016. Trehalose upregulates progranulin expression in human and mouse models of GRN

haploinsufficiency: a novel therapeutic lead to treat frontotemporal dementia. Molecular Neurodegeneration 11, 1–17.

Hong, S., Hwang, D.-Y., Yoon, S., Isacson, O., Ramezani, A., Hawley, R.G., Kim, K.-S., 2007. Functional Analysis of Various Promoters in Lentiviral Vectors at Different Stages of In Vitro Differentiation of Mouse Embryonic Stem Cells. Mol Ther 15, 1630–1639.

Hsu, P.D., Scott, D.A., Weinstein, J.A., Ran, F.A., Konermann, S., Agarwala, V., Li, Y., Fine, E.J., Wu, X., Shalem, O., Cradick, T.J., Marraffini, L.A., Bao, G., Zhang, F., 2013. DNA targeting specificity of RNA-guided Cas9 nucleases. Nat Biotech 31, 827–832.

Iqbal, K., Grundke-Iqbal, I., Smith, A.J., George, L., Tung, Y.C., Zaidi, T., 1989. Identification and localization of a tau peptide to paired helical filaments of Alzheimer disease. Proceedings of the National Academy of Sciences of the United States of America 86, 5646–5650.

Israel, M.A., Yuan, S.H., Bardy, C., Reyna, S.M., Mu, Y., Herrera, C., Hefferan, M.P., Van Gorp, S., Nazor, K.L., Boscolo, F.S., Carson, C.T., Laurent, L.C., Marsala, M., Gage, F.H., Remes, A.M., Koo, E.H., Goldstein, L.S.B., 2012. Probing sporadic and familial Alzheimer's disease using induced pluripotent stem cells. Nature 482, 216–220.

Jo, C., Gundemir, S., Pritchard, S., Jin, Y.N., Rahman, I., Johnson, G.V., 2014. Nrf2 reduces levels of phosphorylated tau protein by inducing autophagy adaptor protein NDP52. Nature communications 5, 3496–3496.

Komatsu, M., Waguri, S., Chiba, T., Murata, S., Iwata, J., Tanida, I., Ueno, T., Koike, M., Uchiyama, Y., Kominami, E., Tanaka, K., 2006. Loss of autophagy in the central nervous system causes neurodegeneration in mice. Nature 441, 880–884.

Komatsu, M., Waguri, S., Koike, M., Sou, Y., Ueno, T., Hara, T., Mizushima, N., Iwata, J., Ezaki, J., Murata, S., Hamazaki, J., Nishito, Y., Iemura, S., Natsume, T., Yanagawa, T., Uwayama, J., Warabi, E., Yoshida, H., Ishii, T., Kobayashi, A., Yamamoto, M., Yue, Z., Uchiyama, Y., Kominami, E., Tanaka, K., 2007. Homeostatic Levels of p62 Control Cytoplasmic Inclusion Body Formation in Autophagy-Deficient Mice. Cell 131, 1149–1163.

Komatsu, M., Waguri, S., Ueno, T., Iwata, J., Murata, S., Tanida, I., Ezaki, J., Mizushima, N., Ohsumi, Y., Uchiyama, Y., Kominami, E., Tanaka, K., Chiba, T., 2005. Impairment of starvation-induced and constitutive autophagy in Atg7-deficient mice. The Journal of Cell Biology 169, 425–434.

Kosik, K.S., Joachim, C.L., Selkoe, D.J., 1986. Microtubule-associated protein tau (tau) is a major antigenic component of paired helical filaments in Alzheimer disease. Proceedings of the National Academy of Sciences of the United States of America 83, 4044–4048.

Kovacs, A., Seglen, P., 1982. Inhibition of hepatocytic protein degradation by inducers of autophagosome accumulation. Acta Biol Med Ger.

Krüger, U., Wang, Y., Kumar, S., Mandelkow, E.-M., 2012. Autophagic degradation of tau in primary neurons and its enhancement by trehalose. Neurobiology of Aging 33, 2291–2305.

Kuma, A., Hatano, M., Matsui, M., Yamamoto, A., Nakaya, H., Yoshimori, T., Ohsumi, Y., Tokuhisa, T., Mizushima, N., 2004. The role of autophagy during the early neonatal starvation period. Nature 432, 1032–1036.

Lei, Z., Brizzee, C., Johnson, G.V.W., 2015. BAG3 facilitates the clearance of endogenous tau in primary neurons. Neurobiology of Aging 36, 241–248.

Levine, B., Kroemer, G., 2008. Autophagy in the Pathogenesis of Disease. Cell 132, 27–42.

Li, J.-F., Norville, J.E., Aach, J., McCormack, M., Zhang, D., Bush, J., Church, G.M., Sheen, J., 2013. Multiplex and homologous recombination-mediated genome editing in Arabidopsis and Nicotiana benthamiana using guide RNA and Cas9. Nat Biotech 31, 688–691.

Li, M., Husic, N., Lin, Y., Christensen, H., Malik, I., McIver, S., LaPash Daniels, C.M., Harris, D.A., Kotzbauer, P.T., Goldberg, M.P., Snider, B.J., 2010. Optimal promoter usage for lentiviral vector-mediated transduction of cultured central nervous system cells. Journal of neuroscience methods 189, 56–64.

Lindwall, G., Cole, R.D., 1984. Phosphorylation affects the ability of tau protein to promote microtubule assembly. Journal of Biological Chemistry 259, 5301–5305.

Lv, X., Jiang, H., Li, B., Liang, Q., Wang, S., Zhao, Q., Jiao, J., 2014. The Crucial Role of Atg5 in Cortical Neurogenesis During Early Brain Development. Scientific Reports 4, 6010.

Mandegar, M.A., Huebsch, N., Frolov, E.B., Shin, E., Truong, A., Olvera, M.P., Chan, A.H., Miyaoka, Y., Holmes, K., Spencer, C.I., Judge, L.M., Gordon, D.E., Eskildsen, T.V., Villalta, J.E., Horlbeck, M.A., Gilbert, L.A., Krogan, N.J., Sheikh, S.P., Weissman, J.S., Qi, L.S., So, P.-L., Conklin, B.R., 2016. CRISPR Interference Efficiently Induces Specific and Reversible Gene Silencing in Human iPSCs. Cell Stem Cell 18, 541–553.

Ma, T., Li, J., Xu, Y., Yu, C., Xu, T., Wang, H., Liu, K., Cao, N., Nie, B., Zhu, S., Xu, S., Li, K., Wei, W., Wu, Y., Guan, K., Ding, S., 2015. Atg5-independent autophagy regulates mitochondrial clearance and is essential for iPSC reprogramming. Nat Cell Biol 17, 1379–1387.

Matsushita, N., Matsushita, S., Hirakawa, S., Higashiyama, S., 2013. Doxycycline-Dependent Inducible and Reversible RNA Interference Mediated by a Single Lentivirus Vector. Bioscience, Biotechnology, and Biochemistry 77, 776–781.

Mizushima, N., 2004. Methods for monitoring autophagy. The International Journal of Biochemistry & Cell Biology 36, 2491–2502.

Mizushima, N., Klionsky, D.J., 2007. Protein Turnover Via Autophagy: Implications for Metabolism. Annu. Rev. Nutr. 27, 19–40.

Nakai, A., Yamaguchi, O., Takeda, T., Higuchi, Y., Hikoso, S., Taniike, M., Omiya, S., Mizote, I., Matsumura, Y., Asahi, M., Nishida, K., Hori, M., Mizushima, N., Otsu, K., 2007. The role of autophagy in cardiomyocytes in the basal state and in response to hemodynamic stress. Nat Med 13, 619–624.

Petiot, A., Ogier-Denis, E., Blommaart, E.F.C., Meijer, A.J., Codogno, P., 2000. Distinct Classes of Phosphatidylinositol 3′-Kinases Are Involved in Signaling Pathways That Control Macroautophagy in HT-29 Cells. Journal of Biological Chemistry 275, 992–998.

Piras, A., Collin, L., Grüninger, F., Graff, C., Rönnbäck, A., 2016. Autophagic and lysosomal defects in human tauopathies: analysis of post-mortem brain from patients with familial Alzheimer disease, corticobasal degeneration and progressive supranuclear palsy. Acta Neuropathologica Communications 4, 22.

Pyo, J.-O., Jang, M.-H., Kwon, Y.-K., Lee, H.-J., Jun, J.-I., Woo, H.-N., Cho, D.-H., Choi, B., Lee, H., Kim, J.-H., Mizushima, N., Oshumi, Y., Jung, Y.-K., 2005. Essential Roles of Atg5 and FADD in Autophagic Cell Death: Dissection of Autophagic Cell Death into Vacuole Formation and Cell Death. Journal of Biological Chemistry 280, 20722–20729.

Qin, J.Y., Zhang, L., Clift, K.L., Hulur, I., Xiang, A.P., Ren, B.-Z., Lahn, B.T., 2010. Systematic Comparison of Constitutive Promoters and the Doxycycline-Inducible Promoter. PLoS ONE 5, e10611.

Raben, N., Hill, V., Shea, L., Takikita, S., Baum, R., Mizushima, N., Ralston, E., Plotz, P., 2008. Suppression of autophagy in skeletal muscle uncovers the accumulation of ubiquitinated proteins and their potential role in muscle damage in Pompe disease. Human Molecular Genetics 17, 3897–3908.

Ran, F.A., Hsu, P.D., Wright, J., Agarwala, V., Scott, D.A., Zhang, F., 2013. Genome engineering using the CRISPR-Cas9 system. Nat. Protocols 8, 2281–2308.

Rodríguez-Martín, T., Cuchillo-Ibáñez, I., Noble, W., Nyenya, F., Anderton, B.H., Hanger, D.P., 2013. Tau phosphorylation affects its axonal transport and degradation. Neurobiology of Aging 34, 2146–2157.

Sanjana, N.E., Shalem, O., Zhang, F., 2014. Improved vectors and genome-wide libraries for CRISPR screening. Nat Meth 11, 783–784.

Sarkar, C., Zhao, Z., Aungst, S., Sabirzhanov, B., Faden, A.I., Lipinski, M.M., 2014. Impaired autophagy flux is associated with neuronal cell death after traumatic brain injury. Autophagy 10, 2208–2222.

Sarkar, S., Davies, J.E., Huang, Z., Tunnacliffe, A., Rubinsztein, D.C., 2007. Trehalose, a Novel mTOR-independent Autophagy Enhancer, Accelerates the Clearance of Mutant Huntingtin and α-Synuclein. Journal of Biological Chemistry 282, 5641–5652.

Schaeffer, V., Lavenir, I., Ozcelik, S., Tolnay, M., Winkler, D.T., Goedert, M., 2012. Stimulation of autophagy reduces neurodegeneration in a mouse model of human tauopathy. Brain 135, 2169–2177.

Seglen, P.O., Gordon, P.B., 1982. 3-Methyladenine: Specific inhibitor of autophagic/lysosomal protein degradation in isolated rat hepatocytes. Proceedings of the National Academy of Sciences of the United States of America 79, 1889–1892.

Shalem, O., Sanjana, N.E., Hartenian, E., Shi, X., Scott, D.A., Mikkelsen, T.S., Heckl, D., Ebert, B.L., Root, D.E., Doench, J.G., Zhang, F., 2014. Genome-Scale CRISPR-Cas9 Knockout Screening in Human Cells. Science 343, 84–87.

Stamer, K., Vogel, R., Thies, E., Mandelkow, E., Mandelkow, E.-M., 2002. Tau blocks traffic of organelles, neurofilaments, and APP vesicles in neurons and enhances oxidative stress. The Journal of Cell Biology 156, 1051–1063.

Stroikin, Y., Dalen, H., Lööf, S., Terman, A., 2004. Inhibition of autophagy with 3-methyladenine results in impaired turnover of lysosomes and accumulation of lipofuscin-like material. European Journal of Cell Biology 83, 583–590.

Suen, D.-F., Narendra, D.P., Tanaka, A., Manfredi, G., Youle, R.J., 2010. Parkin overexpression selects against a deleterious mtDNA mutation in heteroplasmic cybrid cells. Proceedings of the National Academy of Sciences 107, 11835–11840.

Takatsuka, C., Inoue, Y., Matsuoka, K., Moriyasu, Y., 2004. 3-Methyladenine Inhibits Autophagy in Tobacco Culture Cells under Sucrose Starvation Conditions. Plant and Cell Physiology 45, 265–274.

Thoreen, C.C., Sabatini, D.M., 2009. Rapamycin inhibits mTORC1, but not completely. Autophagy 5, 725–726.

Tsuchiya, R., Yoshiki, F., Kudo, Y., Morita, M., 2002. Cell type-selective expression of green fluorescent protein and the calcium indicating protein, yellow cameleon, in rat cortical primary cultures. Brain Research 956, 221–229.

Tsukamoto, S., Kuma, A., Murakami, M., Kishi, C., Yamamoto, A., Mizushima, N., 2008. Autophagy Is Essential for Preimplantation Development of Mouse Embryos. Science 321, 117–120.

Vale, R.D., 2003. The Molecular Motor Toolbox for Intracellular Transport. Cell 112, 467–480.

Voges, D., Zwickl, P., Baumeister, W., 1999. The 26S Proteasome: A Molecular Machine Designed for Controlled Proteolysis. Annu. Rev. Biochem. 68, 1015–1068.

Wang, S., Li, B., Qiao, H., Lv, X., Liang, Q., Shi, Z., Xia, W., Ji, F., Jiao, J., 2014. Autophagy-related gene Atg5 is essential for astrocyte differentiation in the developing mouse cortex. EMBO rep 15, 1053–1061.

Wang, T., Wei, J.J., Sabatini, D.M., Lander, E.S., 2014. Genetic Screens in Human Cells Using the CRISPR-Cas9 System. Science 343, 80–84.

Wang, Y., Mandelkow, E., 2016. Tau in physiology and pathology. Nat Rev Neurosci 17, 22–35.

Warren, N.M., Piggott, M.A., Perry, E.K., Burn, D.J., 2005. Cholinergic systems in progressive supranuclear palsy. Brain 128, 239–249.

Weingarten, M.D., Lockwood, A.H., Hwo, S.Y., Kirschner, M.W., 1975. A protein factor essential for microtubule assembly. Proceedings of the National Academy of Sciences of the United States of America 72, 1858–1862.

Wu, Y., Li, Y., Zhang, H., Huang, Y., Zhao, P., Tang, Y., Qiu, X., Ying, Y., Li, W., Ni, S., Zhang, M., Liu, L., Xu, Y., Zhuang, Q., Luo, Z., Benda, C., Song, H., Liu, B., Lai, L., Liu, X., Tse, H.-F., Bao, X., Chan, W.-Y., A. Esteban, M., Qin, B., Pei, D., 2015. Autophagy and mTORC1 regulate the stochastic phase of somatic cell reprogramming. Nat Cell Biol 17, 715–725.

Wu, Y.-T., Tan, H.-L., Shui, G., Bauvy, C., Huang, Q., Wenk, M.R., Ong, C.-N., Codogno, P., Shen, H.-M., 2010. Dual Role of 3-Methyladenine in Modulation of Autophagy via Different Temporal Patterns of Inhibition on Class I and III Phosphoinositide 3-Kinase. Journal of Biological Chemistry 285, 10850–10861.

Xu, Z.-L., Mizuguchi, H., Ishii-Watabe, A., Uchida, E., Mayumi, T., Hayakawa, T., 2001. Optimization of transcriptional regulatory elements for constructing plasmid vectors. Gene 272, 149–156.

Yamada, K., Holth, J.K., Liao, F., Stewart, F.R., Mahan, T.E., Jiang, H., Cirrito, J.R., Patel, T.K., Hochgräfe, K., Mandelkow, E.-M., Holtzman, D.M., 2014. Neuronal activity regulates extracellular tau in vivo. The Journal of Experimental Medicine 211, 387–393.

Yuan, S.H., Martin, J., Elia, J., Flippin, J., Paramban, R.I., Hefferan, M.P., Vidal, J.G., Mu, Y., Killian, R.L., Israel, M.A., Emre, N., Marsala, S., Marsala, M., Gage, F.H., Goldstein, L.S.B., Carson, C.T., 2011. Cell-Surface Marker Signatures for the Isolation of Neural Stem Cells, Glia and Neurons Derived from Human Pluripotent Stem Cells. PLoS ONE 6, e17540.

Yue, Z., Jin, S., Yang, C., Levine, A.J., Heintz, N., 2003. Beclin 1, an autophagy gene essential for early embryonic development, is a haploinsufficient tumor suppressor. Proceedings of the National Academy of Sciences 100, 15077–15082.